

# Fabrication of two-layer integrated phase mask for single-beam and single-exposure fabrication of three-dimensional photonic crystal

Yuankun Lin,<sup>1\*</sup> Ahmad Harb,<sup>2</sup> Daniel Rodriguez,<sup>2</sup> Karen Lozano,<sup>2</sup> Di Xu,<sup>3</sup> and K. P. Chen<sup>3</sup>

<sup>1</sup>Department of Physics and Geology, University of Texas-Pan American, Edinburg, Texas 78541

<sup>2</sup>Department of Mechanical Engineering, University of Texas-Pan American, Edinburg, Texas 78541

<sup>3</sup>Department of Electrical and Computer Engineering, University of Pittsburgh, Pittsburgh, PA 15261

\*Corresponding author: [linyk@utpa.edu](mailto:linyk@utpa.edu)

**Abstract:** In this paper, we report a new design and fabrication of an integrated two-layer phase mask for five-beam holographic fabrication of three-dimensional photonic crystal templates. The phase mask consists of two layers of orthogonally oriented gratings produced in a polymer. The vertical spatial separation between two layers produces a phase shift among diffractive laser beams, which enables the holographic fabrication of interconnected three-dimensional photonic structures. A three-dimensional photonic crystal template was fabricated using the two-layer phase mask and was consistent with simulations based on the five beam interference. The reported method simplifies the fabrication of photonic crystals and is amendable for massive production and chip-scale integration of three-dimensional photonic structures.

© 2008 Optical Society of American

**OCIS codes:** (090.0090) Holography; (110.5220) Photolithography; (260.3160) Interference; (220.4000) Microstructure fabrication

---

## References and links

1. S. John, "Strong localization of photons in certain disordered dielectric superlattices," *Phys. Rev. Lett.* **58**, 2486-2489 (1987).
2. E. Yablonovitch, "Inhibited Spontaneous Emission in Solid-State Physics and Electronics," *Phys. Rev. Lett.* **58**, 2059-2062 (1987).
3. J. D. Joannopoulos, P. R. Villeneuve, and S. H. Fan, "Photonics crystals: putting a new twist on light," *Nature (London)* **386**, 143-147 (1997).
4. K. M. Ho, C. T. Chan, C. M. Soukoulis, R. Biswas, and M. Sigalas, "Photonic band gaps in three dimensions: New layer-by-layer periodic structures," *Solid State Commun.* **89**, 413-416 (1994).
5. A. Blanco, E. Chomski, S. Grabtchak, M. Ibsate, S. John, S. W. Leonard, C. Lopez, F. Meseguer, H. Miguez, J. P. Mondia, P. Jessica, G. A. Ozin, A. Geoffrey, O. Toader, and H. M. van Driel, "Large-scale synthesis of a silicon photonic crystal with a complete three-dimensional bandgap near 1.5 micrometers," *Nature (London)* **405**, 437-440 (2000).
6. M. Deubel, G. V. Freymann, M. Wegener, S. Pereira, K. Busch, and C. M. Soukoulis, "Direct laser writing of three-dimensional photonic-crystal templates for telecommunications," *Nat. Mater.* **3**, 444-447 (2004).
7. V. Berger, O. Gauthier-Lafaye, and E. Costard, "Photonic band gaps and holography," *J. Appl. Phys.* **82**, 60-64 (1997).
8. M. Campbell, D. N. Sharp, M. T. Harrison, R. G. Denning, and A. J. Turberfield, "Fabrication of photonic crystals for the visible spectrum by holographic lithography," *Nature (London)* **404**, 53-56 (2000).
9. S. Yang, M. Megens, J. Aizenberg, P. Wiltzius, P. M. Chaikin, and W. B. Russel, "Creating periodic three-dimensional structures by multibeam interference of visible laser," *Chem. Mater.* **14**, 2831-2833 (2002).
10. O. Toader, T. Y. M. Chan, and S. John, "Photonic band gap architectures for holographic lithography," *Phys. Rev. Lett.* **92**, 043905/1-4 (2004).
11. D. N. Sharp, A. J. Turberfield, and R. G. Denning, "Holographic photonic crystals with diamond symmetry," *Phys. Rev. B* **68**, 205102-6 (2003).

12. N. D. Lai, W. P. Liang, J. H. Lin, C. C. Hsu, and C. H. Lin, "Fabrication of two- and three-dimensional periodic structures by multi-exposure of two-beam interference technique," *Opt. Express* **13**, 9605-9611 (2005),  
<http://www.opticsexpress.org/abstract.cfm?URI=OPEX-13-23-9605>.
13. M. J. Escuti, J. Qi, and G. P. Crawford, "Tunable face-centered-cubic photonic crystal formed in holographic polymer dispersed liquid crystals," *Opt. Lett.* **28**, 522-524 (2003).
14. Y. K. Pang, J. C. Wai Lee, H. F. Lee, W. Y. Tam, C. T. Chan, and P. Sheng, "Chiral microstructures (spirals) fabrication by holographic lithography," *Opt. Express* **13**, 7615-7620 (2005),  
<http://www.opticsexpress.org/abstract.cfm?URI=OPEX-13-19-7615>.
15. I. Divliansky, T. S. Mayer, K. S. Holliday, and V. H. Crespi, "Fabrication of three-dimensional polymer photonic crystal structures using single diffraction element interference lithography," *Appl. Phys. Lett.* **82**, 1667-1669 (2003).
16. S. Jeon, J.-U. Park, R. Cirelli, S. Yang, C. E. Heitzman, P. V. Braun, P. J. A. Kenis, and J. A. Rogers, "Fabricating complex three-dimensional nanostructures with high-resolution conformable phase masks," *PNAS* **101**, 12429-12434 (2004).
17. Y. Lin, P. R. Herman, and E. L. Abolghasemi, "Proposed single-exposure holographic fabrication of microsphere-type photonic crystal through phase mask techniques," *J. Appl. Phys.* **97**, 096102/1-3 (2005).
18. Y. Lin, P. R. Herman, and K. Darmawikarta, "Design and holographic fabrication of tetragonal and cubic photonic crystals with phase mask: toward the mass-production of three-dimensional photonic crystals," *Appl. Phys. Lett.* **86**, 071117/1-3 (2005).
19. D. Chanda, L. Abolghasemi, and P. R. Herman, "One-dimensional diffractive optical element based fabrication and spectral characterization of three-dimensional photonic crystal templates," *Opt. Express* **14**, 8568-8577 (2006),  
<http://www.opticsinfobase.org/abstract.cfm?URI=oe-14-19-8568>
20. D. Chanda and P. R. Herman, "Phase tunable multilevel diffractive optical element based single laser exposure fabrication of three-dimensional photonic crystal templates," *Appl. Phys. Lett.* **91**, 061122/1-3 (2007).
21. T. Y. M. Chan, O. Toader, and S. John, "Photonic band-gap formation by optical-phase-mask lithography," *Phys. Rev. E* **73**, 046610 (2006).
22. Y. Lin, D. Rivera, Z. Pole, and K. P. Chen, "Five-beam interference pattern controlled through phases and wavevectors for diamondlike photonic crystal," *Appl. Opt.* **45**, 7971-7976 (2006).
23. Y. K. Pang, J. C. Lee, C. T. Ho, and W. Y. Tam, "Realization of woodpile structure using optical interference holography," *Opt. Express* **14**, 9113-9119 (2006),  
<http://www.opticsinfobase.org/abstract.cfm?URI=oe-14-20-9113>
24. H. Miguez, N. Tetreault, B. Hatton, S. M. Yang, D. Perovic, and G. A. Ozin, "Mechanical stability enhancement by pore size and connectivity control in colloidal crystals by layer-by-layer growth of oxide," *Chem. Commun. (Cambridge)* **22**, 2736-2737 (2002).
25. N. Tetreault, G. von Freymann, M. Deubel, M. Hermatschweiler, F. Perez-Willard, S. John, M. Wegener, and G. A. Ozin, "New route to three-dimensional photonic bandgap materials: silicon double inversion of polymer templates," *Adv. Mater.* **18**, 457-460 (2006).
26. Y. Lin and P. R. Herman, "Effect of structural variation on the photonic band gap in woodpile photonic crystal with body-centered-cubic symmetry," *J. Appl. Phys.* **98**, 063104/4 (2005).
27. O. Toader, T. Chan, and S. John, "Photonic band gap synthesis by holographic lithography," *Phys. Rev. Lett.* **92**, 043905/4 (2004).
28. R. Jakubiak, L. V. Natarajan, V. Tondiglia, G. S. He, P. N. Prasad, T. J. Bunning and R. A. Vaia, "Electrically switchable lasing from pyrromethene 597 embedded holographic-polymer dispersed liquid crystals," *Appl. Phys. Lett.* **85**, 6095-6097 (2004).
29. V. P. Tondiglia, L. V. Natarajan, R. L. Sutherland, D. Tomlin, and T. J. Bunning, "Holographic formation of Electro-Optical Polymer-Liquid Crystal Photonic Crystals," *Adv. Mater.* **14**, 187-191 (2002).
30. S. Peng and G. M. Morris, "Efficient implementation of rigorous coupled-wave analysis for surface-relief gratings," *J. Opt. Soc. Am. A* **12**, 1087-1096 (1995).

## 1. Introduction

A photonic crystal is a dielectric medium in which periodic microstructures are formed using high refractive index contrast materials [1, 2]. Since its first introduction in 1987, a large number of applications have been proposed using photonic crystal structures [3]. However, it has been a great challenge to rapidly fabricate large-area and defect-free three-dimensional (3D) photonic crystals at low cost. So far, a number of fabrication techniques such as conventional multilayer stacking of woodpile structures using semiconductor fabrication processes [4], colloidal self-assembly [5], and multi-photon direct laser writing [6], have been employed to produce sub-micron 3D photonic crystals or templates. Holographic lithography based on multi-beam interference has recently been employed to fabricate 3D photonic crystals by exposing a photoresist or polymerizable resin to interference patterns of laser beams [7-23]. This multi-beam interference technique has produced defect free, submicron-

scale structures over large substrate areas [8, 9]. Photonic structures are defined in photoresist by iso-intensity (iso-laser dosage) surfaces of interference patterns [10]. A desired geometrical structure could be obtained by single or multiple exposures [7-9, 11, 12]. The holographic lithography has also been used to produce tunable photonic crystals in a liquid crystal and polymer system [13], and to demonstrate a chiral microstructure in SU-8 photoresist [14]. In the case of positive resist, the overexposed material is then dissolved away in the post-exposure processing. The underexposed region forms a periodic network and acts as a 3D photonic crystal template. For negative photoresists, the underexposed regions can then be selectively removed using a developer while overexposed region becomes polymerized and forms a periodic network for photonic crystal template. The template can then be infiltrated at room temperature with SiO<sub>2</sub> and burned away, leaving behind a daughter “inverse” template [24, 25]. Finally, the daughter template is inverted by infiltration with silicon and selective etching of the SiO<sub>2</sub> [25].

However, fabrication strategies that rely on interference of multiple independent beams have introduced optical complexity when a large number of bulk optical components, such as mirrors, beam splitters, and lenses were used to generate multi-beams. In order to improve the optical setup, diffractive optical elements or phase masks have been introduced to create the interference pattern for the holographic fabrication of photonic crystals [15-21]. When a single beam goes through a diffractive optical element or a phase mask, an interference pattern will be formed behind these optical devices. If designed properly, a single optical element can replace a complex optical setup to generate a desired interference pattern [15-21]. A simple face-centered-cubic structure can be achieved with a single exposure through a two-dimensional phase mask [17]. However, such a structure does not lead to a large photonic band gap comparing with the diamond-like structure. The diamond-like structure not only has a large photonic bandgap but also the bandgap is robust to deviations of the structural parameters from their optimum values [22, 26, 27]. Holographic lithography based on four non-coplanar beams can generate diamond-like structures with beams from all 360° space [27]. Five-beam interference can generate a diamond-like structure with all beams from the same half space [23].

Although the adaptation of single diffractive optical element has significantly simplified the optical setup to generate three or five interfering laser beams, the formation of diamond-like or woodpile structures requires a well-controlled  $\pi$ -phase difference among diffractive laser beams. To achieve this, the woodpile structures have been produced by two independent laser exposures through a one-dimensional phase mask [18, 19], in which the  $\pi$ -phase shift was introduced by a physical displacement of the phase mask between two exposures. This precise displacement on the order of 0.1  $\mu\text{m}$  was achieved using a high precision motion stage, which poses a significant fabrication challenge and is susceptible to the mechanic vibration. Another method to achieve the diamond-like or woodpile structure through five interfering beams is to use polarization effect with a configuration consisting of four linearly polarized side beams arranged symmetrically around a circularly polarized central beam [23].

Chan, *et al.*, have proposed theoretically to “lock” the required phase shift in the mask by fabricating one-dimensional gratings in two layers on the same substrate. The optimized phase shift is determined by the vertical spatial separation between two gratings [21]. Illuminating the phase mask with a normally incident beam produces a five-beam interference pattern which can be used to expose a suitable photoresist and produce a photonic crystal template. One can carefully design the phase mask to manipulate the relations of the interfering beams and thus it can be used to produce photonic crystal templates with diamond-like structures. However no experimental fabrication of such an optical phase mask has been reported to date.

In this paper, we demonstrate an experimental approach to the fabrication of multiple-layer phase mask on a single substrate. The fabricated optical phase mask consisting of two orthogonally oriented gratings has high diffraction efficiencies and generate five-beam interference pattern with a phase relation among the interfering beams. The photonic crystal template is fabricated by exposing a photoresist to the five-beam interference pattern.

## 2. Fabrication of two-layer phase mask

One laser beam (532 nm, 60 mW, Coherent Compass laser) was expanded to a size of 10 mm and separated into two beams using a beam-splitter. A parallel fringe is formed when two laser beams overlap. The spacing  $\Lambda$  between the dark (or bright) fringes is determined by the laser wavelength and interference angle  $\theta$  by the relationship of  $\Lambda = \lambda / (2 \sin \theta)$ . When a photoresist is exposed to the interference pattern and developed, it forms a one-dimensional grating on the substrate. In order to protect the grating formed after laser exposure, liquid crystal was employed to mix with the photoresist. Their inherent phase separation characteristic played a key role in the fabrication of the integrated phase mask described as follows.

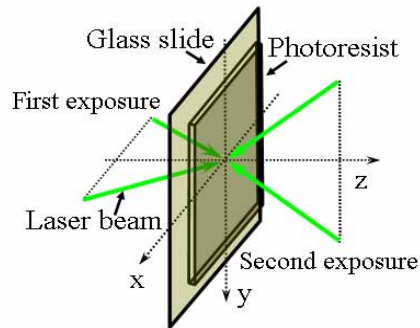


Fig. 1. Scheme of two beam interference for the formation of optical phase mask consisting of two orthogonally oriented gratings in a photoresist.

The photoresist mixtures were similar to a reported formulation (without fatty acid) [28] containing the following components in the specified weight concentrations: dipentaerythritol penta/hexaacrylate (DPHPA) monomer (Aldrich, 65%), BL111 liquid crystal (EMD Chemicals, 25%), a photo initiator rose bengal (0.3%), co-initiator N-phenyl glycine (NPG, 0.5%), chain extender N-vinyl pyrrolidinone (NVP, 9.2%). For the phase mask fabrication, the mixture was spin-coated over a transparent glass slide (Corning) with a typical speed of 4000 rpm for the phase mask fabrication. The thickness of the sample is determined by the spin-coating speed. For such a spin-coating speed of 4000 rpm, the typical thickness of the

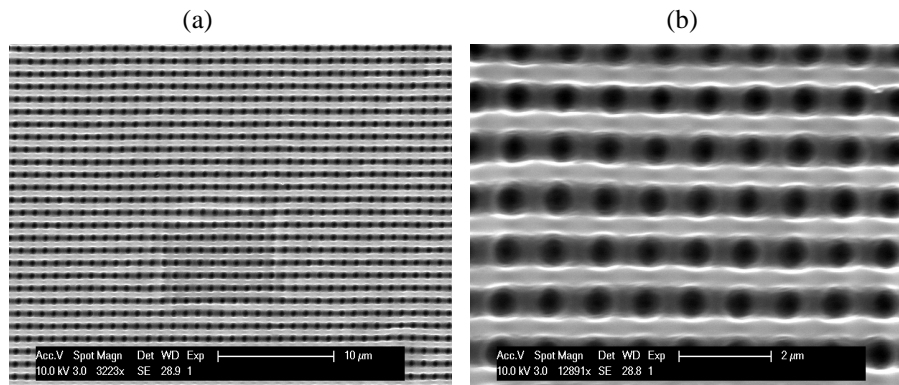


Fig. 2. Scanning electron microscope of the fabricated phase mask showing two layers of grating structure (a), and the enlarged view (b).

sample is 3 microns. Due to a well known polymerization-induced phase separation process [28, 29], the laser exposed sample consists of a periodic distribution of liquid crystal-rich domains, corresponding to the dark regions of the interference pattern, and polymer-rich grating structure. Two laser exposures were performed for the fabrication of phase mask. For the first exposure, two interfering laser beams came from the glass slide side as shown in Fig. 1 and formed the liquid crystal-rich and polymer-rich gratings parallel to the y-direction. The liquid crystal-rich region is much less sensitive to further laser exposure than the polymer-rich region. More laser exposures will induce weak polymerization in the liquid crystal-rich region allowing this region to be washed out during the development. Thus the addition of liquid crystal in the photo-sensitive mixture helps preserve the grating structure produced in the first exposure. The time for first exposure was in the range of 0.5 to 2 seconds. Because the exposure time is short, only the photoresist near the glass-slide (substrate) becomes polymerized. Then the same sample was exposed to the laser interference pattern rotated by 90 degrees and coming from the sample side as shown in the figure. After an exposure in the range of 2 to 4 seconds, a grating parallel to the x-direction is formed. The sample was developed in propylene-glycol-methyl-ether-acetate (PGMEA) (Microchem) for 20 seconds and rinsed in isopropanol.

Figure 2(a) shows the scanning electron microscope (SEM) of the fabricated sample. The SEM shows clearly two layers of grating structures. The top layer has a grating in the horizontal direction. The layer beneath has a grating in vertical direction, orthogonal to the top grating structure. Figure 2(b) shows an enlarged view of the fabricated structure. From the scale bar, the period of the grating was measured to be 1.06  $\mu\text{m}$ . The diffraction angle of the 532 nm laser by the grating was measured to be 31 degrees, corresponding to a grating period of 1.03  $\mu\text{m}$ . These two measurements indicate that the range of the period is in between 1.03 and 1.06  $\mu\text{m}$ .

When a single beam goes through such a phase mask, it is desirable to have five and only five diffracted beams behind the phase mask, namely the (0,0), (0,  $\pm 1$ ) and ( $\pm 1$ , 0) beams [21]. The next lowest order beams are the ( $\pm 1$ ,  $\pm 1$ ) beams. If the phase mask was designed properly, these four beams vanish. The five low order diffracted beams can be described by:

$$\mathbf{E}_{0,0}(\mathbf{r}, t) = \mathbf{E}_{0,0} \cos((k_{0,0} \cdot \mathbf{r} - \omega t + \delta_1)), \quad (1)$$

$$\mathbf{E}_{1,0}(\mathbf{r}, t) = \mathbf{E}_{1,0} \cos((k_{1,0} \cdot \mathbf{r} - \omega t + \delta_1)), \quad (2)$$

$$\mathbf{E}_{-1,0}(\mathbf{r}, t) = \mathbf{E}_{-1,0} \cos((k_{-1,0} \cdot \mathbf{r} - \omega t + \delta_1)), \quad (3)$$

$$\mathbf{E}_{0,1}(\mathbf{r}, t) = \mathbf{E}_{0,1} \cos((k_{0,1} \cdot \mathbf{r} - \omega t + \delta_2)), \quad (4)$$

$$\mathbf{E}_{0,-1}(\mathbf{r}, t) = \mathbf{E}_{0,-1} \cos((k_{0,-1} \cdot \mathbf{r} - \omega t + \delta_2)) \quad (5)$$

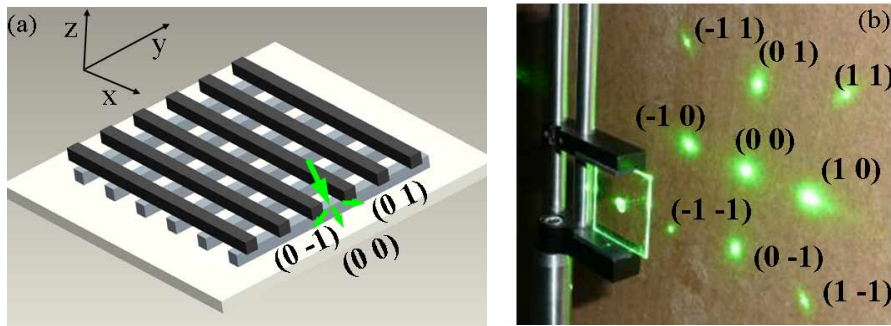


Fig. 3. (a). Scheme of phase mask and diffracted beams by the top grating; (b) Photo of fabricated phase mask and diffracted beams by the phase mask.

where  $k$  and  $\omega$  are the wave vector and angular frequency of the beam, respectively,  $E$  is the constant of electric field strength, and  $\delta$  is the initial phase of the beam. If the initial phases for five beams are the same, the generated interference pattern has face-center-cubic (FCC) or tetragonal (FCT) symmetry [17, 21, 22]. In this study, the initial phases for beams (0, 1) and (0, -1) are the same, but different from those for beams (0, 0), (1, 0), and (-1, 0), i.e. the  $\delta_1$  and  $\delta_2$  are different in the above equations. This is a consequence of the optical path difference developed between (0, 0) and (0, 1) (or (0, -1)) when (0, 0) beam goes in straight line while the (0, 1) or (0, -1) travels along a direction with a diffraction angle before further diffracted by second grating, as shown in Fig. 3(a).

As shown in Fig. 3(b) as an example, when one beam goes through the phase mask, nine diffracted beams can be produced. The beams (1, 0) and (-1, 0) have approximately the same intensity, although the (1, 0) beam spot looks bigger than (-1, 0) caused by a closer distance to the digital camera. Beams (0, 1) and (0, -1) have the same intensity also. The  $(\pm 1, \pm 1)$  beams are very weak and their diffraction angles are larger than the  $(\pm 1, 0)$  and  $(0, \pm 1)$  beams. The beam intensities for (0, 1) and (0, -1) modes might be different from those for beams (1, 0), and (-1, 0), depending on the diffraction efficiency. As an example, one of the fabricated phase masks generates beam intensities with a ratio of 1: 0.68: 0.38: 0.13 for (0, 0), (1, 0), (0, 1) and (1, 1), respectively. The diffraction efficiency is determined by the cycle, depth, and period of the grating structure, the polarization direction of the laser, and the laser wavelength [30]. Experimentally the cycle and depth of the grating structure can be controlled through the weight percentage of photo-initiator, the laser exposure time and the sample development time. The period of the grating can be controlled through the interfering angle of the two laser beams. There is a way to compensate the intensity difference during the exposure of the five-beam interference to the photo-sensitive material. If the polarization of the laser is set to be in  $[1, 0, 0]$  direction, the diffracted beams (1, 0) and (-1, 0) have polarization directions in  $xz$  plane with an angle relative to  $x$ -axis same as the diffraction angle. The diffracted beams (0, 0), (0, 1) and (0, -1) have the same polarization as  $[1, 0, 0]$ .  $\mathbf{E}(\mathbf{r}, \mathbf{t})$  in the above Eqs. (1-5) has the amplitude containing both the intensity and polarization. Thus intensity difference can be compensated by the selection of a polarization for the interference of above five beams when calculating the dot product of two beams.

### 3. Single-beam, single exposure fabrication of photonic crystal template

Using a one-dimensional phase mask, two exposures of the sample to the interference pattern were required to produce a 3D photonic crystal [18]. Using a two-dimensional phase mask, one exposure can produce a 3D photonic crystal [17]. With the two-layer (3D) phase mask produced in this work, not only can one produce a 3D photonic crystal by a single beam and single exposure, but also can introduce the phase shift of the interfering beams. Incorporation of the phase shift for (0, 1) and (0, -1) beams is necessary for the fabrication of 3D photonic crystals with a large photonic band gap [21].

The lab-fabricated phase mask was used to generate a 3D photonic crystal template in the photoresist mixture with a similar formulation to that described above except that the liquid crystal was omitted. The mixture contains (DHPA) monomer (84.9 %), rose bengal (0.4 %), NPG (0.8 %), NVP (13.9 %). The mixture was spin-coated on the glass slide substrate at a speed of 1000 rpm. The thickness is approximately 15 micron. The phase mask generated beam intensities with a ratio of 1: 0.68: 0.38: 0.13 for (0, 0), (1, 0), (0, 1) and (1, 1), respectively. The exposure laser has a wavelength of 532 nm with a polarization in the  $x$ -direction  $[1, 0, 0]$ . As shown in Fig. 4(a), the photonic crystal template can be fabricated in the photoresist by the single beam and single exposure method using the phase mask. The photoresist was placed in a location where five and only five beams overlap and generate the interference pattern. The exposure time was 60 seconds. The exposed photoresist was developed in PGMEA. Figure 4(b) shows a large-scale SEM of the fabricated photonic crystal template. From the theory, the period of the structure in Fig. 4(b) should be the same as the



grating period of the phase mask. The measured average period by SEM is approximately  $1.02\ \mu\text{m}$ , compared with the measured grating period of  $1.06\ \mu\text{m}$  in Fig. 2(b).

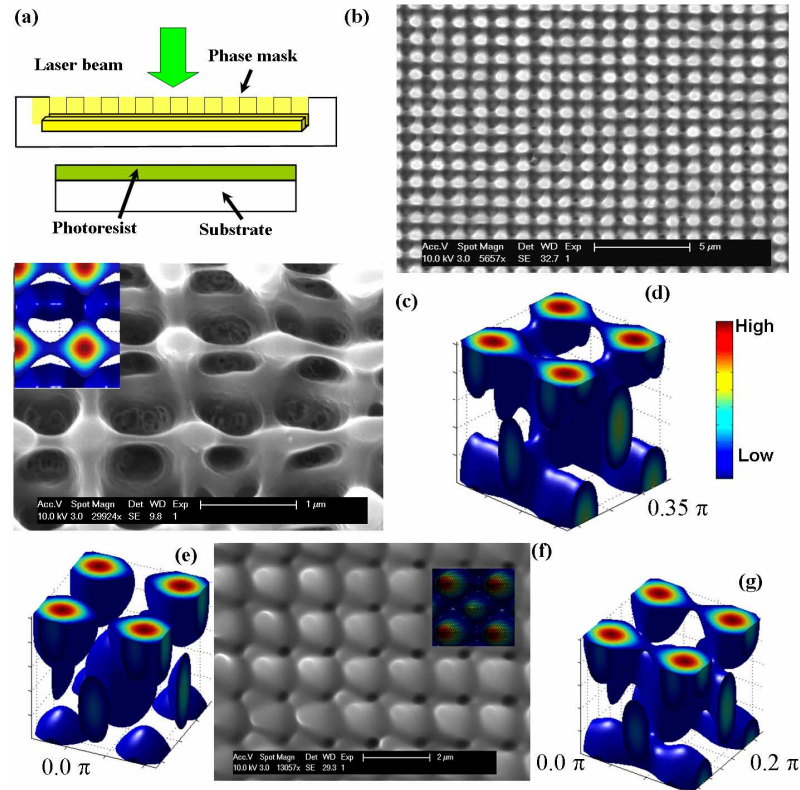


Fig. 4. (a). Scheme of setup for single beam exposure; (b) SEM of photonic crystal template fabricated using the phase mask through single beam and single exposure method; (c) An enlarged view of SEM. The inset is the simulation of five-beam interference pattern; (d-e) 3D pattern of the five-beam interference with  $\delta_1 - \delta_2 = 0.35\pi$  (d) and  $\delta_1 - \delta_2 = 0\pi$  (e); (f) Fabricated structure in SU-8 with  $\delta_1 - \delta_2 = 0\pi$  and simulated intensity pattern as an insert; (g) 3D pattern of the five-beam interference with  $\delta_1 - \delta_2 = 0.2\pi$ .

Figure 4(c) clearly shows a 3D feature of the fabricated structure. The detailed feature of the SEM can be simulated as shown as an insert in Fig. 4(c). The grating period of 1.06 micron was used for the simulation. The beam intensities were set with the values we have measured above, namely, the ratio of beam intensity was set to be 1: 0.68:0.68:0.38:0.38 for (0, 0), (1, 0), (-1, 0), (0, 1), (0, -1) and (1, 1). The polarization of the incident laser was set in the [1, 0, 0] direction. After the diffraction, the polarization for (0, 0), (0, 1) and (0, -1) beams was set in the [1, 0, 0] direction. For (1, 0) and (-1, 0) beams, polarization directions were chosen in xz plane with an angle of 31 degrees relative to x-axis. The maximum phase shift ( $\delta_1 - \delta_2$ ) was estimated to be  $0.47\pi$  based on the sample thickness of 3 microns. A phase shift of  $0.35\pi$  ( $\delta_1 - \delta_2 = 0.35\pi$ ) between the group of (0, 1) and (0, -1) beams and the group of (0, 0), (1, 0), and (-1, 0) beams can simulate the fabricated structure in Fig. 4(c) (see the insert for the simulation). Figure 4(d) shows the 3D view of above simulated structure. As we have stated early, the incorporation of the phase shift for (0, 1) and (0, -1) beams is necessary for the

fabrication of the diamond-like structure. If the phase shift is zero, the low-intensity iso-intensity surface of the five-beam interference looks like spheroid-type FCC or FCT structure as shown in Fig. 4(e). Such a structure is not interconnected and thus is not stable. Under high laser dosage, the structure is interconnected but there is diminished accessibility for the solvent to wash out regions of low intensity exposure. Figure 4(f) shows a SEM of a fabricated FCT structure in SU-8 photoresist under a high laser dosage with a phase shift of zero (the detail of the fabrication in SU-8 will be reported elsewhere). The fabricated structure is in good agreement with a simulated intensity pattern of the interference as shown as an insert in Fig. 4(f). Compared Fig. 4(c) with Fig. 4(f), it is very clear that the fabricated structure through the two layer phase mask is totally different from the fabricated structure with zero phase shift. With a phase shift of  $0.2\pi$ , the spheroids start to interconnect and form diamond-like structure as shown in Fig. 4(g). The perfect phase shift is  $0.5\pi$ . With such a phase shift, the interference pattern has a diamond-like structure as reported in reference 21. The fact that the fabricated structure through the two-layer phase mask can be simulated by an interference pattern with a phase shift and is totally different from the fabricated structure with zero phase shift, indicates that there is the phase shift among beams generated by the two-layer phase mask.

#### 4. Discussion and summary

The described method solved the optical alignment problem that one has faced using two separate one-dimensional phase masks [18]. Alignment of the two interference patterns in 3D space proved difficult in the production of the wood-pile type photonic crystal [18]. This work solves the previously encountered difficulties, because using two-beam interference for the fabrication of the phase mask, there is no issue of alignment as long as the sample is rotated by 90 degrees for the second exposure. Furthermore optical alignment is no longer a concern for the fabrication of the photonic crystal template using the phase mask through single beam and single exposure holographic lithography.

Once the optimal directions, amplitudes, polarizations, and phases are determined, a two-layer phase mask can be designed and fabricated to yield the optimal diffraction condition for the holographic fabrication. The integration of the two-layer phase mask on a single substrate represents a significant improvement toward mass production of 3D photonic structures. Since the two-layer mask can be readily integrated with multiple-layer amplitude mask based IC fabrication, the proposed approaches also provide an avenue for chip-scale integration of the 3D photonic devices with other lightwave and electronic circuit elements.

In summary, we have demonstrated experimentally, for the first time to our best knowledge, the fabrication of a two-layer integrated phase mask consisting of two orthogonally oriented gratings. The phase mask was made by double exposure of the photoresist to the laser interference pattern. The phase separation between liquid crystal and the polymer helps preserve the grating produced in the first exposure. The phase relation among the diffracted beams from the phase mask can be manipulated for the generation of a photonic crystal with a large photonic band gap. The photonic crystal template has been fabricated by single-exposure, single-beam, optical interference lithography through the single integrated phase mask.

#### Acknowledgments

This work is supported by National Science Foundation under awards of CMMI-0609345 (Y. L., and K. L.), DMR-0722754 (Y. L.), and CMMI-0637065 (K. P. C.)